

Comparing mono- and divalent DNA groove binding cyanine dyes—Binding geometries, dissociation rates, and fluorescence properties

Maja Eriksson^{*}, Fredrik Westerlund, Merima Mehmedovic, Per Lincoln, Gunnar Westman, Anette Larsson, Björn Åkerman^{*}

Department of Chemical and Biological Engineering, Chalmers University of Technology, S-412 96 Göteborg, Sweden

Received 27 January 2006; received in revised form 16 March 2006; accepted 19 March 2006

Available online 24 March 2006

Abstract

The unsymmetrical cyanine dyes BOXTO-PRO and BOXTO-MEE were derived from the DNA groove binder BOXTO, by adding a positively charged or a non-ionic hydrophilic tail to BOXTO, respectively. The main objective was to obtain more efficient DNA probes, for instance in electrophoresis and microscopy, by slowing down the dissociation of BOXTO from DNA. The interactions with mixed sequence DNA was studied with fluorescence and absorbance spectroscopy, stopped-flow dissociation and gel electrophoresis. Both the derivatives are groove bound as BOXTO, and have similar fluorescence properties when bound to mixed sequence DNA in free solution. BOXTO-PRO exhibits a slower dissociation than BOXTO from DNA, whereas the dissociation rate for BOXTO-MEE is faster and, unexpectedly independent of the ionic strength. During gel electrophoresis both BOXTO-PRO and BOXTO-MEE exhibit a faster dissociation rate than BOXTO. Still, BOXTO-PRO seems to be a good alternative as DNA probe, especially for applications in free solution where the dissociation is slower than for the corresponding intercalator TOPRO-1.

© 2006 Elsevier B.V. All rights reserved.

Keywords: Cyanine dyes; Groove binding to mixed sequence DNA; Dissociation kinetics; Spectroscopy; Gel electrophoresis

1. Introduction

Asymmetric cyanine dyes are useful spectroscopic probes for DNA in microscopy [1–3], electrophoresis [4] and PCR [5] because of a strongly enhanced fluorescence quantum yield when bound to DNA compared to free dye. Temperature and viscosity studies [6] indicate that the fluorescence enhancement is due to quenching of an intramolecular rotation. This mechanism is of a different nature compared to other fluorescence-based DNA probes, such as ethidium bromide [7] and ruthenium complexes [8], where DNA-binding instead leads to protection from solvent quenching.

Most of the presently used cyanine dyes bind to DNA by intercalation between the base pairs [9–11]. Recently, there have been several efforts to develop groove binding cyanine dyes [12–16] because this mode of binding perturbs the DNA helix less than intercalation does [17,18]. Recent studies of several derivatives of the intercalating dyes BO and TO [13,14,19] have shown that the TO-derivate BOXTO is a promising candidate as a DNA probe, as it exhibits a strong preference for groove binding and has a 50-fold increase in fluorescence quantum yield upon binding to random sequence DNA [14].

Fluorescence microscopy and gel electrophoresis often relies on non-equilibrium staining conditions in order to reduce the background fluorescence from free dye. With the aim to slow down the dissociation from DNA [20], the divalent BOXTO-PRO (Fig. 1) was derived by addition of a positively charged 3-propyl trimethyl ammonium chloride tail to BOXTO. This approach was inspired by how intercalating ethidium bromide was modified to obtain propidium iodide which has higher

^{*} Corresponding authors. Maja Eriksson is to be contacted at Tel.: +46 31 7723053; fax: +46 31 7723858. Björn Åkerman, Tel.: +46 31 7723052; fax: +46 31 7723858.

E-mail addresses: maja.eriksson@chalmers.se (M. Eriksson), baa@chalmers.se (B. Åkerman).

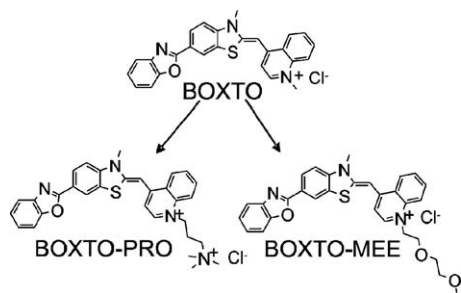


Fig. 1. The structures of **BOXTO-PRO** (4-[(3-methyl-6-(benzoxazole-2-yl)-2,3-dihydro-(benzo-1,3-thiazole)-2-methylidene)]-1-(3-trimethylammonium-propyl)-quinolinium dichloride) and **BOXTO-MEE** (4-[(3-methyl-6-(benzoxazole-2-yl)-2,3-dihydro-(benzo-1,3-thiazole)-2-methylidene)]-1-methoxyethoxyethyl quinolinium chloride), obtained from **BOXTO** (4-[6-(benzoxazol-2-yl)-(3-methyl)-2,3-dihydro-(benzo-1,3-thiazole)-2-methylidene]-1-methyl-quinolinium chloride).

affinity and slower dissociation than the monovalent ethidium [21]. Here we investigate if the added charge has a corresponding retarding effect on the dissociation of groove-binders.

Furthermore, in our experience, BOXTO has a tendency to aggregate and to bind to surfaces. With the goal to reduce such effects, we also studied the derivative BOXTO-MEE (Fig. 1) that contains a polar (but non-ionic) methoxyethoxyethyl tail. The monovalent charge of BOXTO-MEE means that we can investigate how a hydrophilic modification affects the interaction with DNA, without altering the electrostatic interactions between BOXTO and DNA.

We here present studies of how the modifications that give BOXTO-PRO and BOXTO-MEE affect the interaction with mixed sequence DNA, regarding the binding mode and the fluorescence properties of the DNA bound dyes. We also characterize how the dissociation from DNA is altered, both in free solution and inside agarose gels where the dyes are used for DNA-detection during electrophoresis.

2. Experimental

2.1. Materials

BOXTO-PRO and BOXTO-MEE were prepared by reacting equimolar amounts of quinolinium salt and benzothiazolium salt in methylene chloride in the presence of triethylamine as previously described [14]. The two quinolinium salts were prepared by reacting two mole-equivalents quinoline with one mole-equivalent 3-bromopropyl trimethylamine or triethyleglycol tosylate, respectively, at 130 °C for 3 h. After cooling, the precipitate was washed with acetone to give the salt (see Supplementary material). A more detail description of the synthesis will be presented elsewhere (Karlsson, H.J., manuscript in preparation). BOXTO was synthesized as described previously [14]. The dyes were stored as stock solutions in DMSO at −20 °C. The concentration of the dyes in the working solutions was determined by a parallel and identical dilution of the DMSO stock solution in buffer and methanol, using an extinction coefficient of 70 000 M^{−1} cm^{−1} in methanol at

510 nm as determined by weighing (See Supporting material). This approach was used since the extinction coefficient in aqueous solution was uncertain due to dimerisation of free dye, which was avoided in methanol. YO was synthesized as previously described [22], whereas TOPRO-1, BOPRO-1, YOPRO-1, and YOYO-1 were purchased from Molecular Probes. The concentrations were determined in phosphate buffer by using the following extinction coefficients: YO (66 000 cm^{−1} M^{−1} at 482 nm), YOPRO-1 (66 000 cm^{−1} M^{−1} at 482 nm), TOPRO-1 (63 000 cm^{−1} M^{−1} at 506 nm), BOPRO-1 (63 000 cm^{−1} M^{−1} at 451 nm), and YOYO-1 (96 100 cm^{−1} M^{−1} at 457 nm) [6,20]. Double stranded calf thymus DNA (ctDNA) with an average size of 6000 base pairs, and monodisperse DNA from bacteriophage T5 (122 kilo base pairs) were purchased from Sigma-Aldrich. The DNA concentration was determined by using an extinction coefficient of 6600 M^{−1} cm^{−1} per base at 260 nm. Agarose and sodium dodecyl sulphate (SDS) were purchased as powders from Sigma-Aldrich and VWR International, respectively.

2.2. Spectroscopic measurements

All spectroscopic measurements of dye–DNA complexes were performed at room temperature (22 °C) in 5 mM sodium phosphate buffer (pH 7.0) by adding an increasing amount of ctDNA to a sample with a fixed dye concentration. If nothing else is stated, spectral band widths were 2.0 nm for absorption, 2.5 nm for emission and excitation, 1.0 nm for linear dichroism (LD), and 4.0 nm for circular dichroism (CD).

The absorbance spectra were measured using a Cary 4000 Bio-UV–Vis spectrophotometer (Varian) and the fluorescence excitation and emission spectra were measured using a Varian Cary Eclipse spectrofluorimeter. The fluorescence enhancements for the dyes when bound to DNA were calculated as the ratio between the integrated areas of the emission spectra in presence and absence of DNA, respectively. The relative fluorescence quantum yields of the bound dyes were calculated from the areas of the integrated emission spectra. In both cases the integrated emission was corrected for the absorbance at the excitation wavelength.

Linear dichroism (LD) is the difference in absorption of light polarized perpendicular and parallel to a macroscopic orientation axis. Linear dichroism measurements were performed on a Jasco-720 spectropolarimeter where flow orientation of the DNA complexes was achieved by using a flow Couette cell with an outer rotating cylinder. Calf thymus DNA is long enough to be oriented with its long axis preferentially in the flow direction of the Couette cell. Since the DNA bases mainly absorb light polarized perpendicularly to this axis, the result is a negative LD signal with its maximum value at 260 nm. Ligands that bind to DNA will also exhibit a nonisotropic orientation and consequently give rise to positive or negative LD signals depending on the binding geometry to DNA and on the orientation of the transition moments within the dyes. A reduced LD (LD^r) spectrum is obtained by dividing the LD spectrum with the corresponding isotropic absorbance spectrum, from which the angle (α) between the transition moment of the ligand and the

DNA helix axis can be calculated [23] (see Supporting material).

Circular dichroism spectra of the DNA dye complexes were measured on a Jasco-810 spectropolarimeter. Magnetic CD (MCD) spectra of free dye in methanol were measured by equipping the Jasco-720 spectropolarimeter with a permanent magnet, as described previously [24].

2.3. Dye dissociation in free solution

The dissociation of the dyes from ctDNA in free solution was monitored by capturing the dissociated dye molecules in SDS micelles, using a computer controlled stopped-flow module SFM-3 coupled to a power supply MPS-52 (Bio Logic). The DNA dye samples (100 μ l) were rapidly mixed with an equal volume of an aqueous solution of SDS. After mixing, the concentration of dye and DNA base pairs was 2.5 μ M and 50 μ M, respectively. The dissociation of the dyes from DNA was measured by following the decline in fluorescence intensity (delay time 3.9 ms). A Xenon–Mercury arc lamp coupled to a monochromator was used to excite the DNA dye complex at its absorbance maximum and the emission decay was measured by using a long pass filter with a 540 nm cutoff. The dissociation kinetics were evaluated at various concentrations of NaCl in the range of 6–205 mM at a constant concentration of SDS (52 mM), as well as with varied concentrations of SDS (8–50 mM) at a constant concentration of salt (106 mM). The dissociation rate constants were determined by fitting the emission data to a bi-exponential decay:

$$I(t) = I_0 + A_1 e^{-k_1 t} + A_2 e^{-k_2 t}. \quad (1)$$

2.4. Dissociation during gel electrophoresis

The rate of dye dissociation from monodisperse double stranded bacteriophage T5 DNA during constant field (7.5 V/cm) gel electrophoresis was measured in agarose gels (1 wt.%) by running the samples in submarine electrophoresis cells in TBE buffer (50 mM Tris, 50 mM sodiumborate, 1.25 mM EDTA, pH=8.2). Each sample (24 μ l) contained DNA at a concentration of 19 μ M base pairs and the dye at a ratio of 0.1 (dye/base pair). The dissociation of the dyes from DNA was monitored by following the decrease in fluorescence intensity of the DNA bands, through scanning of the gels in a FluorImager gel scanner 595 (Molecular Dynamics) 10 times during the electrophoresis (240 min). The zone-integrated emission intensities were obtained with the image evaluation program Image Quant 5.0 and the dissociation half-times were evaluated from the decay of the zone intensities.

3. Results

For the sake of comparison with previous studies [14,20], the new results on BOXTO-PRO and BOXTO-MEE are complemented with earlier results on BOXTO throughout the Results and Discussion sections.

3.1. Absorbance measurements

The absorbance spectra of the three dyes in buffer solution and bound to ctDNA are presented in Fig. 2. The free dyes (solid lines) exhibit a broad absorption band with a peak at 460–475 nm, and a red-shifted shoulder. As discussed below, the peak at the blue side of the spectra indicates that free BOXTO-PRO and BOXTO-MEE (and BOXTO) form dimers (or higher aggregates) in aqueous solution. The shoulder becomes more pronounced in the order BOXTO-PRO, BOXTO-MEE and BOXTO. In methanol, by contrast, all the dyes exhibit a reversed spectral shape, with the major peak at the red side of the absorption band (Supporting material), indicating that aggregation is absent in this solvent.

As DNA was added to the aqueous dye solutions, the absorbance spectrum changed with time during about 1 h at room temperature, presumably due to an initial binding of dye dimers that subsequently rearrange on the DNA helix (Results not shown). All the results presented in this study were obtained from samples that had reached binding equilibrium, as monitored by absorbance.

When the dyes bind to ctDNA (Fig. 2, dashed lines) the absorbance spectra change significantly compared to for free

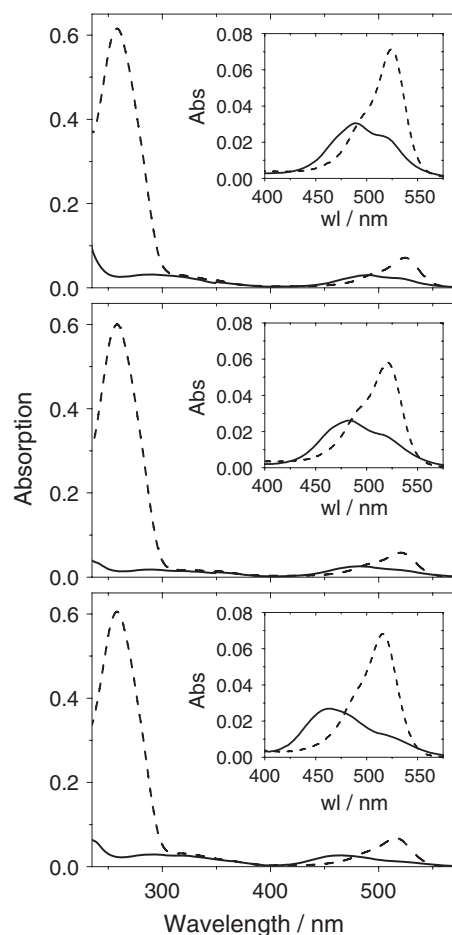


Fig. 2. Absorbance spectra of BOXTO-PRO (top panel), BOXTO-MEE (middle), and BOXTO (bottom) free in buffer solution (solid lines) and bound to ctDNA (dashed lines). [DNA base pair]=53 μ M, [dye]=1.5 μ M.

dyes. There is an overall increase in peak absorbance in the visible region and a red shift in all three cases. The absorbance spectra of the three dyes bound to DNA are very similar.

3.2. LD and CD measurements

Fig. 3 shows the LD spectra of BOXTO-PRO (top), BOXTO-MEE (middle) and BOXTO (bottom panel) bound to ctDNA. All dyes have a positive LD in the visible region, providing a strong indication for non-intercalative binding. The LD amplitude for BOXTO-MEE (main Fig. 3) is seen to be considerably smaller compared to BOXTO-PRO and BOXTO. The LD in the DNA absorption band at 260 nm is negative, as expected from the perpendicular orientation of the bases to the helix axis in the B-form DNA. The LD spectra in the visible region for BOXTO-PRO and BOXTO-MEE are of similar shape as the isotropic absorbance (see insets in Fig. 3), but there are marked red shifts of about 12 and 14 nm respectively, which both are larger than for BOXTO (5 nm). The varying degree of spectral shifts between LD and absorbance for the three dyes indicates the presence of two bound species, as discussed below.

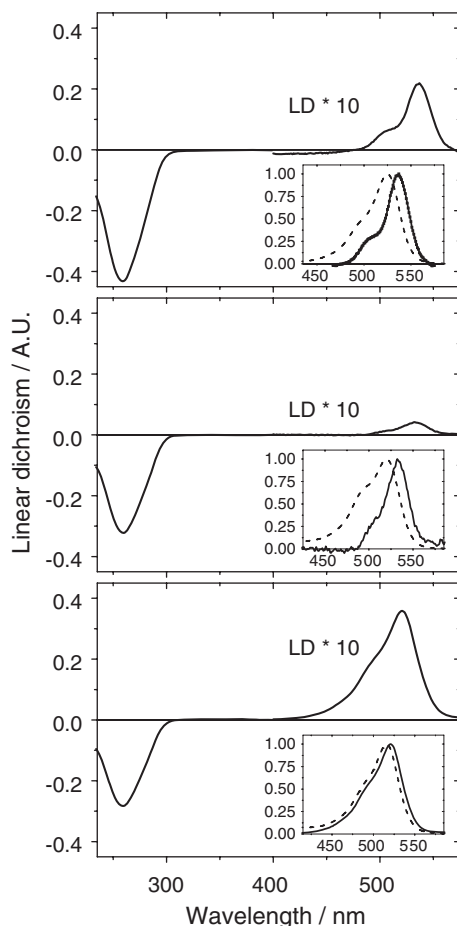


Fig. 3. LD spectra of BOXTO-PRO (top panel), BOXTO-MEE (middle) and BOXTO (bottom) bound to ctDNA. Note that the LD signals (A.U. = absorbance units) are multiplied by a factor of 10 above 400 nm. The insets show normalized LD (solid lines), and isotropic absorbance spectra (dashed lines) for the dyes bound to DNA. [dye] = 8 μ M and [DNA base pair] = 134 μ M.

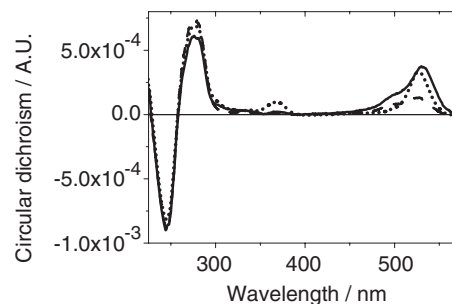


Fig. 4. CD spectra of BOXTO-PRO (solid line), BOXTO-MEE (dashed line) and BOXTO (dotted line) bound to ctDNA. [dye] = 10 μ M, and [DNA base pair] = 150 μ M.

Fig. 4 shows the CD spectra of the three dyes when bound to ctDNA. The bisignate CD spectrum around 260 nm is characteristic for B-form DNA. Both BOXTO-PRO and BOXTO-MEE exhibit a positive induced CD in the visible region, in agreement with the observation for BOXTO. The intensities of the CD peaks are almost equal for BOXTO-PRO and BOXTO, but only half that value for BOXTO-MEE. The strength of the DNA-induced CD of the dyes can be quantified by the ratio $CD/A_{iso} = \Delta\epsilon/\epsilon$ at the wavelength of maximum CD. We obtain $\Delta\epsilon/\epsilon = 7.8 \times 10^{-4}$ for BOXTO-PRO and 4.4×10^{-4} for BOXTO-MEE, compared to 7.3×10^{-4} for BOXTO (see Supporting material).

The shapes of the CD spectra are similar to the absorbance spectra of the DNA dye complexes, but as was the case with LD, the CD maxima are shifted. The major CD peak is red shifted by 5 and 9 nm for BOXTO-PRO and BOXTO-MEE respectively, a shift that is smaller than in LD. However for BOXTO the CD peak is red shifted more than the LD peak (9 nm compared to 5 nm). Notably, neither BOXTO-PRO nor BOXTO-MEE exhibit any detectable CD peak around 370 nm, in contrast to BOXTO.

The chromophore of the dyes was investigated by measuring the MCD spectrum of BOXTO-MEE in methanol. In the visible region the MCD spectrum has a similar shape as the absorption spectrum (results not shown). Importantly it does not exhibit the bisignate shape expected if the absorption band corresponds to two electronic transitions with different directions [24]. The different tail structures of the three dyes are not expected to affect their electronic properties, as supported by the very similar absorption spectra in methanol (Supporting material). The absorbance, LD and CD spectra will therefore be interpreted based on the assumption that a single electronic transition is responsible for the absorption band of the BOXTO chromophore in the visible region.

3.3. Fluorescence measurements

Excitation spectra of BOXTO-PRO, BOXTO-MEE, and BOXTO bound to ctDNA are presented in Fig. 5, where they are compared to the corresponding absorbance spectra. The absorbance and the excitation spectra are very similar for all three dyes, suggesting that all forms of bound dye molecules are

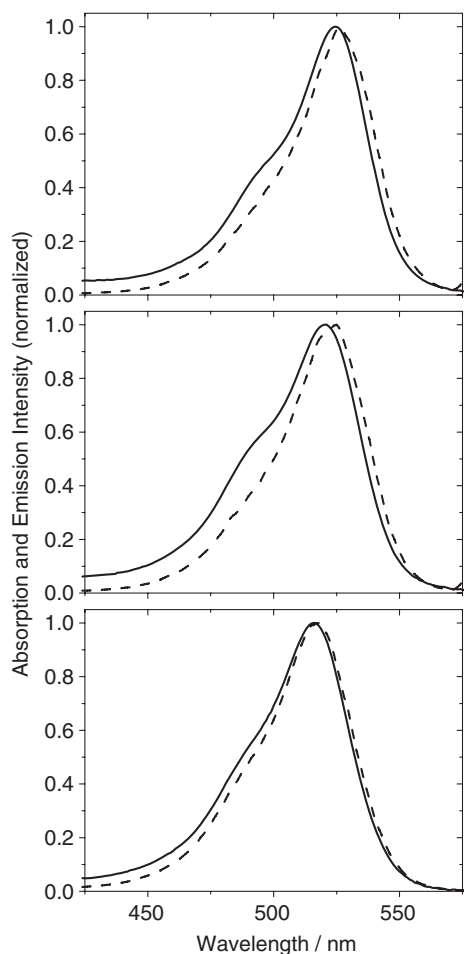


Fig. 5. Normalized absorbance (solid lines) and excitation spectra (dotted lines) of BOXTO-PRO (top panel), BOXTO-MEE (middle), and BOXTO (bottom) bound to ctDNA. The emission intensity was measured at 590 nm for all dyes. [dye] = 1.5 μ M, and [DNA bp] = 53 μ M.

similarly emissive, despite that LD and CD indicate that there are two binding modes.

BOXTO-PRO and BOXTO-MEE, as well as BOXTO, display a substantial increase in fluorescence intensity upon binding to ctDNA. The fluorescence intensity compared to free dye (see Materials section) is enhanced by a factor of 77 for BOXTO-PRO and 48 for BOXTO-MEE, whereas for BOXTO it is enhanced 165 times. The lower fluorescence enhancement with BOXTO-PRO and BOXTO-MEE is mainly an effect of the stronger fluorescence in the non-bound state of these dyes. The quantum yields for the bound forms are 0.80 for BOXTO-PRO and 0.83 for BOXTO-MEE relative to that of bound BOXTO.

3.4. Dissociation in free solution

In accordance with earlier results on BOXTO [20], the dissociation of BOXTO-PRO and BOXTO-MEE from ctDNA was satisfactorily described by a bi-exponential decay (Eq. (1)). The fits and determined rate constants are given in Supporting material. Fig. 6 shows the two rate constants for BOXTO-PRO and BOXTO-MEE plotted versus the ionic strength as varied by addition of NaCl (6–205 mM). For BOXTO-PRO both the

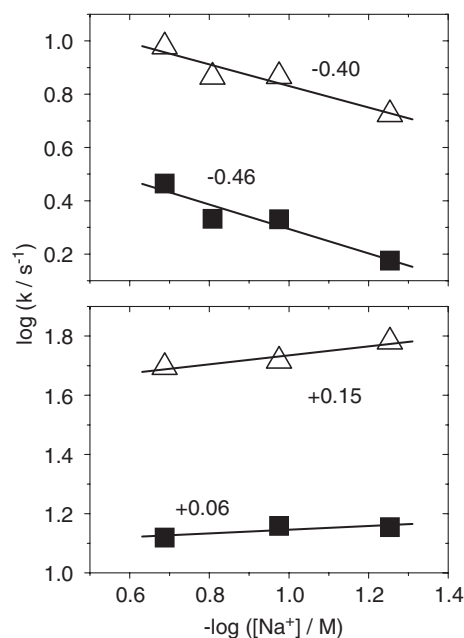


Fig. 6. The effect of NaCl concentration on the two rate constants for the dissociation (open triangles = k_1 , solid squares = k_2) of BOXTO-PRO (top panel) and BOXTO-MEE (bottom) from ctDNA at a constant concentration of SDS (52 mM). [dye] = 2.5 μ M, [DNA bp] = 50 μ M.

dissociation rate constants increase with increasing salt concentration. In the logarithmic plots in Fig. 6 (motivated by counterion shielding theory, see below) the slopes are -0.40 and -0.46 for the fast and the slow rate constants respectively. By contrast, for BOXTO-MEE the dissociation rates are essentially independent of salt concentration. (The fast and slow rate constants in fact exhibit small positive slopes of $+0.15$ and $+0.06$, respectively). In terms of absolute rates, BOXTO-PRO dissociates 5–10 times slower than BOXTO-MEE, depending on salt concentration. The salt dependencies of the rate constants, including BOXTO, are summarized in Table 1.

Fig. 7 shows the relative decay amplitude $A_1/(A_1 + A_2)$ for the fast component of the dissociation plotted versus the negative logarithm of the salt concentration. The contributions from the fast and slow components are almost equal at high ionic strength for both BOXTO-PRO and BOXTO-MEE, and the importance of the fast component decreases weakly with decreasing salt concentration. For BOXTO the fast process is of

Table 1

The slopes for the plots of $\log [k_i \text{ (s}^{-1}\text{)}]$ versus $-\log [\text{NaCl}]$ in Figs. 6 and 8

	Experimental ^a			Predicted
	BOXTO-PRO	BOXTO-MEE	BOXTO ^b	Groove binding ^c
k_1	-0.40	$+0.15$	-0.32	
k_2	-0.46	$+0.06$	-0.26	
k_{app}	-0.51	-0.01	-0.42	
				$-0.76 (+1)$
				$-1.52 (+2)$

^a k_1 is the fast and k_2 is the slow rate constant for the dissociation from ctDNA, k_{app} = the average rate constant according to Eq. (2).

^b From [20].

^c From [30]; number in parenthesis represents the charge of dye.

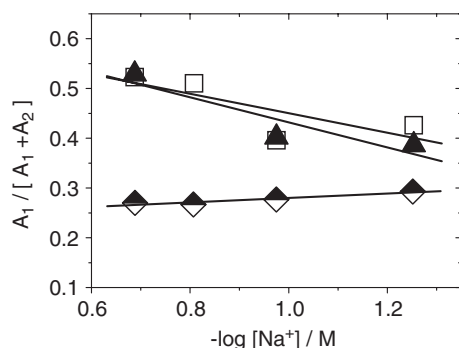


Fig. 7. The relative amplitude of the fast rate constant of the dissociation of BOXTO-PRO (open squares), BOXTO-MEE (solid triangles) and BOXTO (half-filled diamonds) from ctDNA [20] from ctDNA. Lines are guide to the eye only.

less importance, but its weight increases weakly with decreasing salt concentration.

A useful parameter when applications of these dyes are considered is the average dissociation rate constant:

$$k_{\text{app}} = \frac{A_1}{A_1 + A_2} k_1 + \frac{A_2}{A_1 + A_2} k_2 \quad (2)$$

Fig. 8 presents the calculated k_{app} plotted versus the ionic strength for BOXTO-PRO, BOXTO-MEE and BOXTO. The divalent intercalator TOPRO-1 that most closely resembles BOXTO-PRO is also included [20]. The average rate constant summarizes the behavior reported above: BOXTO-PRO dissociates somewhat slower than BOXTO, and BOXTO-MEE is seen to dissociate much faster than both BOXTO-PRO and BOXTO, but slight slower than TO-PRO. The slope of k_{app} versus the ionic strength decreases in the order TOPRO-1, BOXTO-PRO, BOXTO and BOXTO-MEE (Table 2).

3.4.1. SDS effect on the kinetics

A previous study [25] showed that in the case of tetravalent DNA binding dyes such as YOYO, the apparent rates of dissociation measured by SDS sequestering are affected by the surfactant concentration. However, that study also showed that

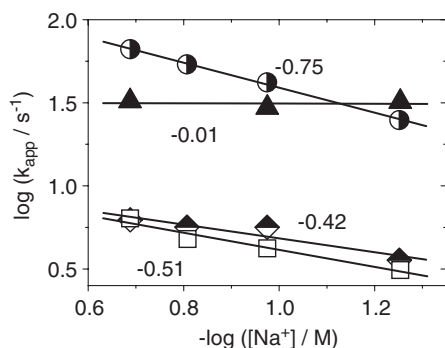


Fig. 8. The logarithm of the average rate constant (k_{app}) versus the negative logarithm of $[\text{NaCl}]$ for the dissociation of BOXTO-PRO (open squares), BOXTO-MEE (solid triangles), BOXTO (half filled diamonds) [20], and TOPRO-1 (half filled circles) [20], from ctDNA. $[\text{dye}] = 2.5 \mu\text{M}$, $[\text{DNA bp}] = 50 \mu\text{M}$, and $[\text{SDS}] = 52 \text{ mM}$.

Table 2

Dissociation half-times during migration in gel electrophoresis (in minutes) and in free solution (in seconds) at $[\text{Na}^+] = 56 \text{ mM}$

Dye	$t_{1/2} (\text{gel})^a$ ($\pm \text{S.E.}$) (min)	$t_{1/2} (\text{sol})^b$ (s)	Ratio 10^{-5}^c
BOXTO-PRO	66 ^d (± 5)	0.22	0.18
BOXTO-MEE	44 ^d (± 4)	0.022	1.20
BOXTO	132 ^e (± 1)	0.19 ^f	0.41
YO	21 ^d (± 4)	n.d.	n.d.
YOPRO-1	158 ^e (± 91)	n.d.	n.d.
YOYO-1	317 min ^e (± 47)	n.d.	n.d.
TOPRO-1	249 ^e (± 6)	0.03 ^g	5.34

^a The average dissociation half-time $t_{1/2} (\text{gel})$ from phage T5 DNA during gel electrophoresis ($N=4$, standard errors $= \pm \text{S.E.}$).

^b The effective half-times $t_{1/2} (\text{sol}) = \ln 2 / k_{\text{app}}$ for the dissociation from ctDNA in free solution at $[\text{Na}^+] = 56 \text{ mM}$.

^c The ratio between the half-times $[t_{1/2} (\text{gel}) / t_{1/2} (\text{sol})]$.

^d The half-times determined from plots of $\ln[I/I_0]$ vs. time.

^e The half-times determined from linear plots of I vs. time.

^f Previously calculated to 0.17 [20]. New corrected analysis of the data gave 0.19.

^g From [20].

for ethidium bromide, with only one positive charge and a much faster dissociation from ctDNA, no effect of surfactant concentration was observed, in agreement with earlier studies [21]. Therefore the rate of dissociation for divalent BOXTO-PRO and monovalent BOXTO-MEE at different surfactant concentrations was investigated by varying the SDS concentration at a constant background concentration of NaCl (106 mM). As was the case with the dissociations at varied NaCl concentration, the decays were satisfactorily fitted by two exponentials. Fig. 9 shows the logarithm of the average rate constant (k_{app}) (Eq. (2)) versus the negative logarithm of the SDS concentration.

The very weak slope (-0.02) observed for BOXTO-PRO can arguably be ascribed to the increase in sodium ion concentration when SDS is added, considering that the slope is as large as -0.51 when sodium ions are added as NaCl (Fig. 8). The weak effect of surfactant concentration indicates that the dissociation is too fast to be catalyzed by SDS, as was the case with ethidium bromide. We conclude that the rate constants measured by SDS sequestering (Fig. 6) are representative for the inherent rates in free solution. With BOXTO-MEE the slope with SDS (-0.1) is

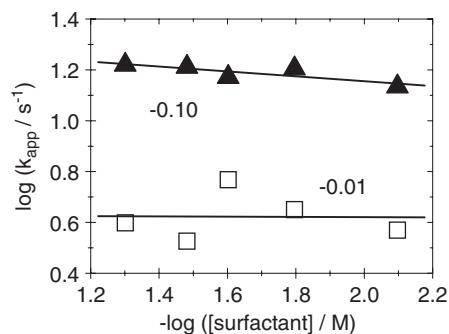


Fig. 9. The logarithm of average rate constant k_{app} (Eq. (2)) versus the negative logarithm of the $[\text{SDS}]$ for the dissociation of BOXTO-PRO (open squares) and BOXTO-MEE (solid triangles) from ctDNA at fixed concentration of NaCl (106 mM). $[\text{dye}] = 2.5 \mu\text{M}$, $[\text{DNA bp}] = 50 \mu\text{M}$.

in fact stronger than with NaCl (-0.01), but it should be noted that the latter slope is unexpectedly small. Notably, SDS catalysis does not seem likely since BOXTO-MEE dissociates considerably faster than BOXTO-PRO (Fig. 8).

3.5. Electrophoretic dissociation

One possible application of the new dyes is as DNA probes in gel electrophoresis. Therefore the dissociation rates of BOXTO-MEE and BOXTO-PRO during migration in gel electrophoresis were compared with BOXTO and the intercalator TOPRO-1. In addition, the intercalators monovalent YO, divalent YOPRO-1 and tetravalent YOYO-1 were added to the study, with all samples evaluated in the same gel. The dissociation half-times were calculated from the decay in fluorescence intensity of the sample zones with time (see Supporting material), and are summarized in Table 2 together with the average dissociation half-times in free solution.

All dyes dissociate much faster in free solution than during migration in gel electrophoresis. BOXTO-PRO, BOXTO-MEE and YO exhibit an exponential decay of the fluorescence intensity during electrophoresis, whereas the more slowly dissociating dyes exhibit an essentially linear decrease in fluorescence intensity with time (Supporting material).

4. Discussion

4.1. Aqueous solubility of the free dyes

One goal with this study was to modify BOXTO in order to decrease its tendency to form aggregates in aqueous solution, by adding either a positively charged tail (BOXTO-PRO) or a hydrophilic (but nonionic) tail (BOXTO-MEE). The absorbance spectra in methanol indicate that all three dyes exist as monomers in that solvent (see Supporting material). By contrast, the absorbance spectra of all three dyes free in aqueous solution (Fig. 2) exhibit a reversed spectral shape compared to that measured in methanol. A similarly reversed spectral shape was observed for the homodimer YOYO in aqueous solution, when compared to the corresponding monomer YOPRO [6]. This observation was interpreted as an enforced stacking of the YO chromophores when they are linked together in the dimer, as supported by the fact that YOYO and YOPRO have very similar spectra in methanol. These observations indicate that both BOXTO-PRO and BOXTO-MEE form dimers (or higher aggregates) in water in spite of the added tail groups.

It is thus clear that the modifications in BOXTO-PRO and BOXTO-MEE did not fully eliminate the tendency to form aggregates. However, the shoulder on the red side of the absorbance spectra (Fig. 2, solid) is enhanced with BOXTO-MEE and even more so with BOXTO-PRO, which suggests that the tail had some effect in increasing the solubility especially if it is charged. This fact may explain our qualitative observation that BOXTO-PRO has the advantage of exhibiting a lower tendency than BOXTO to adsorb to the walls of cuvettes and test tubes.

4.2. DNA binding mode

4.2.1. All three dyes bind primarily as monomers

The absorbance spectra of BOXTO-PRO, BOXTO-MEE and BOXTO bound to DNA (Fig. 2) are very similar, indicating that they all bind to DNA in a similar fashion. In fact, the appearance of the absorbance spectra for the bound dyes are of similar shape to the spectra for the dyes free in methanol (Supporting material), suggesting that they bind primarily as monomers.

The monomeric binding of BOXTO-PRO and BOXTO-MEE to DNA is supported by the CD spectra in Fig. 4, since there is no indication of the bisignate exciton CD that is characteristic for interactions between closely bound dyes like for the TO derivative BETO [14] and the known groove binder DAPI [26]. However, the CD band at 370 nm (Fig. 4, dotted) suggests that exciton interactions do occur between BOXTO molecules. Our previous study [14] showed that the intensity of this CD peak increases as the mixing ratio dye/basepair is increased (at constant dye concentration), as is expected if it is caused by BOXTO molecules binding in close proximity to each other. Furthermore, an analysis of the CD shifts (see below) suggests that for BOXTO the expected negative CD component of the exciton couplet is hidden under the induced CD of the individual monomers.

The interactions between closely bound BOXTO molecules (that cause the exciton CD) is most likely accidental, since the absorption spectrum of bound BOXTO (Fig. 2, dashed lines) does not exhibit any stronger tendency than BOXTO-PRO or BOXTO-MEE to have the reversed spectral shape typical of dimerised or aggregated dyes (Fig. 2, solid lines). That BOXTO-PRO and BOXTO-MEE have no observable tendency to form such CD-detected dye pairs (at similar binding ratios) suggests that the added tails interfere so that bound dye molecules do not come as close to each other as with BOXTO.

4.2.2. Two bound modes for all three dyes

BOXTO-PRO and BOXTO-MEE both exhibit a positive LD in the visible region when bound to ctDNA (Fig. 3), and this similarity to BOXTO indicates that they all bind in the grooves of DNA. However, the substantial shift of the LD peak compared to the isotropic absorbance peak for BOXTO-PRO (Fig. 3 top, inset) is not consistent with one bound form of the dye, since in the latter case the LD spectrum should have the same shape as the absorption spectrum. The same conclusion can be made from the CD spectrum (Fig. 4), although in this case the shift compared to the absorbance is smaller. Notably, the presence of free dye cannot explain the difference in shape between LD and CD, since both techniques only monitor bound dye. We therefore propose that BOXTO-PRO binds to DNA in two different ways. One form is groove bound with a large red shift of the absorption spectrum, a strong induced CD, and a positive LD. The second binding mode has a smaller red shift in absorbance, a weaker CD, and an orientation with respect to DNA that results in a less positive LD. This hypothesis is strongly supported by the observation that the CD spectrum can be reconstructed by using the observed isotropic absorbance

and LD spectra (under the condition that their shapes are constant but that their magnitude can vary) for the bound dyes, as required if all three types of spectra are linear combinations of the spectral contributions from each of the two bound forms (Fig. 10). Furthermore, LD spectra at different binding ratios show consistent changes in shape (Supporting material), as expected if there are two bound forms of the dye.

With BOXTO-MEE we observe similar shifts in CD and LD as with BOXTO-PRO, and the same resolution analysis of the three spectra supports that BOXTO-MEE binds in two different manners similar to the ones observed with BOXTO-PRO. These results on the BOXTO-derivatives lead us to perform a more detailed analysis of the LD and CD data for the BOXTO-parent (Figs. 3 and 4) as well, albeit the LD shift is much less accentuated for this dye. The analysis shows that also the binding of BOXTO is best described by two bound forms similar to BOXTO-PRO and BOXTO-MEE, only that for BOXTO the second (less shifted mode) now exhibits a slightly more positive LD.

4.2.3. The geometry of the first binding mode

The first binding mode (with the largest red shift) most likely corresponds to binding in one of the grooves. A value of $\alpha = 41^\circ$ for the angle between the transition moment in BOXTO-PRO and the helix axis of DNA was calculated from LD^r at the red edge of the absorption band (where this binding mode dominates the spectrum, see Supporting material). This angle

supports groove binding, since it is close to the value $44\text{--}49^\circ$ for the known minor groove-binder DAPI [26,27]. It is likely that the transition moment of the BOXTO chromophore is directed essentially along the long axis of the molecule. The α -values obtained for BOXTO-MEE ($\alpha = 39^\circ$) and for BOXTO ($\alpha = 29^\circ$) are similar albeit smaller than for BOXTO-PRO (i.e. more parallel to the helix axis). Notably, if these dyes bind in the minor groove, the calculated angles suggest that they would have to distort the DNA helix, which is in disagreement with that there are no detectable DNA perturbations when BOXTO binds to supercoiled circular DNA, as monitored by an unwinding assay [28]. One possibility is therefore that the dyes bind in the wider major groove, which allows a larger range of binding angles.

The positive sign of the induced CD (Fig. 4) further supports that the first binding mode of all three dyes is groove binding [29], and the CD intensities ($\Delta\epsilon/\epsilon$ in Table S1 in Supporting material) are of the magnitudes expected for groove binders.

4.2.4. The geometry of the second binding mode

The exact geometry of the second binding mode (with the smaller spectral shift) cannot be ascertained from the spectral resolution analysis. The lower LD amplitude on the blue side of the absorption band suggests that the angle between the long axis of the dye and the helix axis is larger (i.e. less parallel to the helix axis) than for ordinary groove binders. Intercalation is very unlikely, however, because neither BOXTO-PRO [28], nor BOXTO [13] unwind negatively supercoiled circular DNA. That the LD^r of the second binding mode is close to zero suggests that the DNA-bound dye in this binding mode has a comparatively low degree of structural order, such as random binding on the surface of the DNA.

BOXTO exhibits a significant deviation between observed and reconstructed CD around 490 nm, in contrast to the good agreement observed with BOXTO-PRO and BOXTO-MEE (Fig. 10, right panels). (In fact, the left panels show this effect directly in the experimental spectra, because the CD for BOXTO deviates from the CD spectrum of the other dyes by lacking the shoulder on the blue side of the band). The fact that the reconstructed CD overestimates the amplitude suggests that the experimental spectrum has a counteracting negative contribution. We tentatively ascribe this component as the negative part of an exciton couplet for BOXTO where the positive component is observed around 370 nm (Fig. 4).

4.3. Affinity for DNA

The slightly slower dissociation of BOXTO-PRO than BOXTO (Fig. 8) suggests that the affinity for DNA is somewhat higher for BOXTO-PRO. BOXTO-MEE exhibits a considerably faster dissociation than the other two dyes, but it is difficult to estimate a relative affinity from this result, since the association rates are not necessarily comparable. The unexpectedly low sensitivity to ionic strength in the dissociation rate for BOXTO-MEE indicates that it dissociates by another route than BOXTO and BOXTO-PRO.

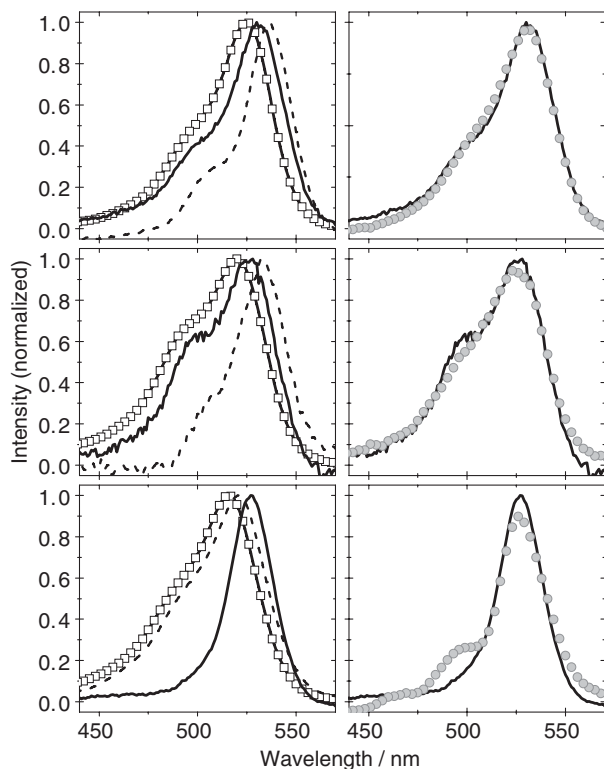


Fig. 10. Normalized absorbance (open squares), LD (dashed lines), and CD (solid lines) spectra of BOXTO-PRO (left top panel), BOXTO-MEE (left middle), and BOXTO (left down) bound to ctDNA. The corresponding right panel shows the best fit of the linear combinations of the LD and absorbance spectra (grey circles) to the CD spectra (solid lines).

The fluorescence intensities when bound to DNA are quite similar for the three dyes (after correction for absorbance the ratios are 0.80 for BOXTO-PRO and 0.83 BOXTO-MEE when compared to BOXTO). This observation indicates that under our conditions (regarding mixing ratio and ionic strength) the relative amount of bound dye is essentially the same for all three dyes. The strong overlap between the absorption and excitation spectra (Fig. 5) also supports that almost all molecules are bound in all three cases, since the presence of (low-emitting) free dye would result in a deviation between these two types of spectra.

4.4. Dissociation in free solution

The approximate linear dependencies between the dissociation rate and the ionic strength that both BOXTO-PRO and BOXTO exhibit in the log–log plot (Fig. 8) is in agreement with theoretical predictions by Wilson and co-workers [21,30]. However, the magnitude of the slope for BOXTO-PRO (−0.51) is well below the predicted value of −1.52 for a groove bound divalent ligand (Table 1), an observation which reinforces our earlier result that the slope for BOXTO (−0.42) is considerably lower than the predicted value of −0.76 for a monovalent groove binder. These deviations are particularly interesting because the theory has been successful in predicting the effect of ionic strength on the dissociation of groove bound DAPI in poly(dA–dT)₂, and of several mono- and divalent intercalators [21,30], including the intercalator TOPRO-1 (slope −0.79) that is structurally closely related to BOXTO-PRO [20].

It is particularly interesting that BOXTO-MEE has a slope as low as −0.01, which is even smaller than the slope for BOXTO (−0.42) even though the two dyes have the same charge. The insensitivity to ionic strength observed for BOXTO-MEE suggests that there is a second (counteracting) effect of the added NaCl. The methoxyethoxyethyl group that constitutes the tail of BOXTO-MEE is known to have an affinity for cations, such as sodium [31–33]. One possibility is that an increase in NaCl concentration favours a fraction of the dye molecules to acquire an extra positive charge by chelating a sodium ion, which could partly offset the screening effect of the added salt. However, BOXTO-MEE is far from optimal for imaging applications because the rate of dissociation is considerably faster than for BOXTO (albeit still slower than for the related divalent intercalator TOPRO-1) [20].

Interestingly, the observation of two bound forms may be related to the fact that the dissociation of all three dyes is biexponential. The fast dissociation and weak slope in Fig. 8 for BOXTO-MEE indicates that BOXTO-MEE dissociates by another mechanism than BOXTO and BOXTO-PRO.

4.5. Electrophoretic dissociation

The dissociation during electrophoretic migration of DNA dye complexes in gels was studied to investigate if the slower dissociation of BOXTO-PRO compared to BOXTO in free solution (Fig. 8) manifests itself in this application. We find that BOXTO-MEE dissociates faster than both BOXTO-PRO and BOXTO in electrophoresis, seemingly consistent with the faster

dissociation in free solution. However, BOXTO-PRO dissociates faster in the gel than both BOXTO and the corresponding intercalator TOPRO-1, while in free solution BOXTO-PRO exhibits the slowest dissociation of these three dyes.

It is reasonable that the decrease in fluorescence in the gel does not correspond to a single event of dye dissociation from DNA, given that the half-times in the gels are 5 orders of magnitude larger than in free solution (Table 2). Apparent stabilization of protein DNA complexes in gels has been ascribed to a cage effect [34], by which the gel matrix slows down the diffusion of the dissociated ligand and enhances its probability of re-association to the target. However, the dye molecules we study here are small compared to proteins, and so small compared to the average pore radius of the agarose gel (250 nm) that the gel matrix can be expected to have negligible effect on their diffusion [35]. We are presently investigating theoretically whether the apparent life-time of the complex instead is governed by the rate by which the dyes leave the DNA zone by electrophoretic migration in the direction opposite to the DNA molecules. If it is assumed that the dyes undergo many dissociation and association events during the process of leaving the zone (Åkerman, Larsson, in preparation) the fluorescence is predicted to decrease with a half-time $t_{1/2}$ (see Supporting material):

$$t_{1/2} = \frac{L_0}{2v_F} (1 + K[S]) \quad (3)$$

where L_0 is the length of the sample zone, v_F is the electrophoretic velocity of the non-bound dye (in the gel), K is the equilibrium binding constant for the dye to DNA and $[S]$ is the effective concentration of free binding sites on the DNA molecules in the zone. Notably, in this model it is the ratio of association and dissociation rate constants (as combined in K), rather than the dissociation rate by itself that controls the effective half-time in the gel. The free velocity of non-bound dye is $v_F = Eq/f$, where E is the field strength, q the charge and f the friction coefficient of the dye. The increasing half-times in the gel for the “homologue” series YO, YOPRO and YOYO (Table 2), is in qualitative agreement with Eq. (3) because the affinity for DNA increases in this order, whereas the ratio q/f is expected to be comparable for all the three dyes. This interpretation is also consistent with previous electrophoresis studies of TO and TOTO [36] and ethidium bromide and its corresponding dimer [37]. Quantitative comparison between BOXTO, BOXTO-PRO, BOXTO-MEE and TOPRO-1 therefore has to wait for the affinity constants to be determined. Another fact that has to be taken into account is interaction with the gel matrix, due to the limited water solubility of the BOXTO-type of dyes. Occasional binding to the gel would increase the apparent friction coefficient. This may explain why the more hydrophilic BOXTO-PRO has a shorter effective half-time in the gel than BOXTO.

5. Conclusions

The primary conclusion from this work is that when BOXTO is extended with a charged or non-ionic polar tail,

the groove binding mode to DNA of BOXTO is retained, and the fluorescence properties are preserved. Notably, a second and less oriented bound form of the dyes becomes more prominent when the tails are present, but since this form also is non-intercalating, BOXTO-PRO may be a useful DNA probe in fluorescence applications where helix perturbation is a disadvantage. One example is when cyanine dyes are used as spectroscopic probes on the DNA organisation inside bacteriophages (Eriksson et al., submitted), where extension of the already strongly packed DNA may affect dye binding. The low sensitivity of BOXTO-MEE-dissociation to ionic strength may also be useful in biological systems, such as gellan gels. The commonly required divalent cations tend to increase dye-dissociation so that even bisintercalators such as YOYO cannot be used in microscopy [38]. However, for microscopy applications the overall rate of dissociation of BOXTO-MEE has to be reduced, perhaps by a dimer-strategy. In general the BOXTO chromophore is an interesting spectral probe for studies of DNA binding, since its emission properties are robust and insensitive to binding geometry, whereas the absorption properties including LD and CD are.

Acknowledgements

Dr. Marcus Wilhelmsson is thankfully acknowledged for assistance in experiments and for helpful discussions. Dr. Jonas Karlsson is acknowledged for the synthesis of BOXTO and for helpful assistance in the initiation of the project.

Appendix A. Supplementary data

Supplementary data associated with this article can be found, in the online version, at [doi:10.1016/j.bpc.2006.03.009](https://doi.org/10.1016/j.bpc.2006.03.009).

References

- [1] J. Han, H.G. Craighead, Separation of long DNA molecules in a microfabricated entropic trap array, *Science* 288 (2000) 1026–1029.
- [2] T.T. Perkins, D.E. Smith, S. Chu, in: T.Q. Nguyen, H.-H. Kausch (Eds.), *Flexible Polymer Chains in Elongational Flow*, Springer, 1999, pp. 283–334.
- [3] S.B. Smith, P.K. Aldridge, J.B. Callis, Observation of individual DNA molecules undergoing gel electrophoresis, *Science* 243 (1989) 203–206.
- [4] S.C. Benson, R.A. Mathies, A.N. Glazer, Heterodimeric DNA-binding dyes designed for energy transfer: stability and applications of the DNA complexes, *Nucleic Acids Res.* 21 (1993) 5720–5726.
- [5] M. Bengtsson, H.J. Karlsson, G. Westman, M. Kubista, A new minor groove binding asymmetric cyanine reporter dye for real-time PCR, *Nucleic Acids Res.* 31 (2003) e45/1–e45/5.
- [6] C. Carlsson, A. Larsson, M. Jonsson, B. Albinsson, B. Norden, Optical and photophysical properties of the oxazole yellow DNA probes YO and YOYO, *J. Phys. Chem., B* 98 (1994) 10313–10321.
- [7] J.I. Olmsted, D.R. Kearns, Mechanism of ethidium bromide fluorescence enhancement on binding to nucleic acids, *Biochemistry* 16 (1977) 3647–3654.
- [8] Y. Jenkins, A.E. Friedman, N.J. Turro, J.K. Barton, Characterization of dipyrrophenazine complexes of ruthenium(II): the light switch effect as a function of nucleic acid sequence and conformation, *Biochemistry* 31 (1992) 10809–10816.
- [9] F. Johansen, J.P. Jacobsen, ¹H NMR studies of the bis-intercalation of a homodimeric oxazole yellow dye in DNA oligonucleotides, *J. Biomol. Struct. Dyn.* 16 (1998) 205–222.
- [10] A. Larsson, C. Carlsson, M. Jonsson, B. Albinsson, Characterization of the binding of the fluorescent dyes YO and YOYO to DNA by polarized light spectroscopy, *J. Am. Chem. Soc.* 116 (1994) 8459–8465.
- [11] Rye Hays, S. Yue, Stephen Wemmer, David, E. Quesada, Mark, A. Haugland, Richard, P. Mathies, Glazer Alexander, N., Stable fluorescent complexes of double-stranded DNA with bis-intercalating asymmetric cyanine dyes: properties and applications, *Nucleic Acids Res.* 20 (1992) 2803–2812.
- [12] R. Cao, C.F. Venezia, B.A. Armitage, Investigation of DNA binding modes for a symmetrical cyanine dye trication: effect of DNA sequence and structure, *J. Biomol. Struct. Dyn.* 18 (2001) 844–856.
- [13] H.J. Karlsson, P. Lincoln, G. Westman, Synthesis and DNA binding studies of a new asymmetric cyanine dye binding in the minor groove of [poly(dA–dT)]₂, *Bioorg. Med. Chem.* 11 (2003) 1035–1040.
- [14] H.J. Karlsson, M. Eriksson, E. Perzon, B. Åkerman, P. Lincoln, G. Westman, Groove-binding unsymmetrical cyanine dyes for staining of DNA: syntheses and characterization of the DNA-binding, *Nucleic Acids Res.* 31 (2003) 6227–6234.
- [15] A.L. Mikheikin, A.L. Zhuze, A.S. Zasedatelev, Binding of symmetrical cyanine dyes into the DNA minor groove, *J. Biomol. Struct. Dyn.* 18 (2000) 59–72.
- [16] H. Zipper, H. Brunner, J. Bernhagen, F. Vitzthum, Investigations on DNA intercalation and surface binding by SYBR Green I, its structure determination and methodological implications, *Nucleic Acids Res.* 32 (2004) e103/1–e103/10.
- [17] I. Tessmer, C.G. Baumann, M.G. Skinner, J.E. Molloy, J.G. Hoggett, S.B. Tendler, S. Allen, Mode of drug binding to DNA determined by optical tweezers force spectroscopy, *J. Mod. Opt.* 50 (2003) 1627–1636.
- [18] J.E. Coury, J.R. Anderson, L. McFail-Isom, L.D. Williams, L.A. Bottomley, Scanning force microscopy of small ligand-nucleic acid complexes: Tris(*o*-phenanthroline)ruthenium(II) as a test for a new assay, *J. Am. Chem. Soc.* 119 (1997) 3792–3796.
- [19] H.J. Karlsson, M. Bergqvist, P. Lincoln, G. Westman, Syntheses and DNA-binding studies of a series of unsymmetrical cyanine dyes: structural influence on the degree of minor groove binding to natural DNA, *Bioorg. Med. Chem.* 12 (2004) 2369–2384.
- [20] M. Eriksson, H.J. Karlsson, G. Westman, B. Åkerman, Groove-binding unsymmetrical cyanine dyes for staining of DNA: dissociation rates in free solution and electrophoresis gels, *Nucleic Acids Res.* 31 (2003) 6235–6242.
- [21] W.D. Wilson, C.R. Krishnamoorthy, Y.H. Wang, J.C. Smith, Mechanism of intercalation: ion effects on the equilibrium and kinetic constants for the interaction of propidium and ethidium with DNA, *Biopolymers* 24 (1985) 1941–1961.
- [22] L.G.S. Brooker, G.H. Keyes, W.W. Williams, Color and constitution: V. The absorption of unsymmetrical cyanines. Resonance as a basis for a classification of dyes, *J. Am. Chem. Soc.* 64 (1942) 199–210.
- [23] B. Nordén, M. Kubista, T. Kurucsev, Linear dichroism spectroscopy of nucleic-acids, *Q. Rev. Biophys.* 25 (1992) 51–170.
- [24] M. Kubista, B. Åkerman, B. Albinsson, Characterization of the electronic structure of 4',6-diamidino-2-phenylindole, *J. Am. Chem. Soc.* 111 (1989) 7031–7035.
- [25] F. Westerlund, L.M. Wilhelmsson, B. Norden, P. Lincoln, Micelle-sequestered dissociation of cationic DNA-intercalated drugs: unexpected surfactant-induced rate enhancement, *J. Am. Chem. Soc.* 125 (2003) 3773–3779.
- [26] M. Kubista, B. Åkerman, B. Norden, Characterization of interaction between DNA and 4',6-diamidino-2-phenylindole by optical spectroscopy, *Biochemistry* 26 (1987) 4545–4553.
- [27] A. Larsen, S. Goodsell, D. Cascio, K. Grzeskowiak, Dickerson, The structure of DAPI bound to DNA, *J. Biomol. Struct. Dyn.* 7 (1989) 477–491.
- [28] M. Eriksson, M. Mehmedovic, G. Westman, B. Åkerman, Time-resolved electrophoretic analysis of mobility shifts for dissociating DNA ligands, *Electrophoresis* 26 (2005) 524–532.

- [29] M. Kubista, B. Åkerman, B. Norden, Induced circular dichroism in nonintercalative DNA–drug complexes: sector rules for structural applications, *J. Phys. Chem.* 92 (1988) 2352–2356.
- [30] W.D. Wilson, F.A. Tanious, H.J. Barton, R.L. Jones, K. Fox, R.L. Wydra, L. Strekowski, DNA sequence dependent binding modes of 4',6-diamidino-2-phenylindole (DAPI), *Biochemistry* 29 (1990) 8452–8461.
- [31] Craine, Leslie H. Greenblatt, Jeremy Woodson, Sarah Hortelano, Edwin Raban, Morton, Stereochemistry in trivalent nitrogen compounds. 39. Configurational biasing of tertiary amide ionophores by alkali metal chelation, *J. Am. Chem. Soc.* 105 (1983) 7252–7255.
- [32] M. Jayakannan, S. Ramakrishnan, Solution cation-binding properties of segmented polyethylene oxide—A ¹³C NMR spectroscopic study, *J. Polym. Sci.* 38 (2000) 2635–2644.
- [33] G.W. Gokel, O. Murillo, J.S. Bradshaw, R.M. Izatt, A.V. Bordunov, C.Y. Zhu, J.K. Hathaway, *Comprehensive Supramolecular Chemistry*, Volume 1: Molecular Recognition: Receptors for Cationic Guests, Elsevier Science, New York, 1996.
- [34] J.R. Cann, Theoretical studies on the mobility-shift assay of protein–DNA complexes, *Electrophoresis* 19 (1998) 127–141.
- [35] B. Åkerman, in: H.S. Nalwa (Ed.), *Handbook of Surfaces and Interfaces of Materials*, Academic press, San Diego, 2001, pp. 431–479.
- [36] S.C. Benson, P. Singh, A.N. Glazer, Heterodimeric DNA-binding dyes designed for energy transfer: synthesis and spectroscopic properties, *Nucleic Acids Res.* 21 (1993) 5727–5735.
- [37] N. Glazer, K. Peck, Mathies, A stable double-stranded DNA–ethidium homodimer complex: application to picogram fluorescence detection of DNA in agarose gels, *Proc. Natl. Acad. Sci. U. S. A.* 87 (1990) 3851–3855.
- [38] M. Markström, K.D. Cole, B. Åkerman, DNA electrophoresis in gellan gels. The effect of electroosmosis and polymer additives, *J. Phys. Chem., B* 106 (2002) 2349–2356.